Geophysical Research Letters

RESEARCH LETTER
10.1029/2026GL122705

Impacts of Deforestation-Driven Rainfall Reductions on Amazonia Forest Stability

Luís Gustavo Cattelan[1], Marina Hirota[2,3], Jessica C. A. Baker[4], Jefferson Gonçalves De Souza[5], Ana Paula Dutra Aguiar[6], Tainá Oliveira Assis[6], Chris Huntingford[7], Eddy Robertson[8], Stephen Sitch[5], and Emanuel Gloor[1]

[1]School of Geography, University of Leeds, Leeds, UK, [2]Department of Physics, Group IpES, Universidade Federal de Santa Catarina (UFSC), Centro de Ciências Físicas e Matemáticas (CFM), Campus Universitário, Florianópolis, Brazil, [3]Universidade Estadual de Campinas, Instituto de Biologia, Departamento de Botânica, Campinas, Brazil, [4]School of Earth and Environment, University of Leeds, Leeds, UK, [5]University of Exeter, Exeter, UK, [6]Earth System Science Center (CCST), National Institute for Space Research (INPE), Ministry of Science, Technology and Innovation (MCTI), São José dos Campos, Brazil, [7]UK Centre for Ecology and Hydrology, Wallingford, UK, [8]Met Office Hadley Centre, Exeter, UK

Abstract The stability of Amazonian vegetation is strongly influenced by land–atmosphere feedbacks. It has been hypothesized that deforestation-induced precipitation decline may lead to widespread forest decline across the entire basin. Using a moisture-tracking model, we quantify how deforestation across South America alters downwind rainfall and affects forest stability. We find widespread forest collapse will not result from deforestation-induced precipitation changes alone. However, we identify key hotspots of vulnerability, including forests in southwestern Amazonia which could transition to non-forest ecosystems in response to upwind deforestation (affecting 81% of the Rondônia state). Western Amazonia and the eastern Amazonia-Cerrado transition zone emerge as key conservation hotspots, where forest loss produces the strongest downwind impacts on vegetation stability. Conversely, restoration in northeast Amazonia could enhance regional rainfall and improve ecosystem stability. Overall, our findings underscore the importance of preserving Amazonia's continental-scale moisture connectivity to safeguard both local ecosystem and broader hydroclimatic stability.

Plain Language Summary Rainfall in the Amazon is strongly influenced by the forest itself. Trees release water into the atmosphere through evapotranspiration, which helps generate rain both locally and in regions downwind. Because of this feedback, there is concern that deforestation could reduce rainfall enough to push parts of the Amazon toward a drier, savanna-like ecosystem. Using a model that tracks how moisture moves through the atmosphere, we examined how deforestation across South America affects rainfall and forest stability. Our results show that deforestation-driven rainfall reductions alone are unlikely to cause a complete collapse of the Amazon forest. However, some regions-especially southwestern Amazônia and the border between the Amazon and Cerrado (known as MATOPIBA)-are highly vulnerable because they depend heavily on moisture from upwind forests. Conversely, reforestation in eastern Pará could help increase rainfall and support forest recovery. These results highlight where conservation and restoration actions would be most effective in maintaining rainfall and forest resilience across the Amazon.

Key Points:

- Deforestation-driven rainfall decline does not cause a basin-wide Amazon tipping point but increases regional vulnerability
- Southwestern Amazônia and MATOPIBA emerge as key hotspots where forest loss most destabilizes downwind ecosystems
- Targeted reforestation in eastern Pará could enhance rainfall recycling and strengthen Amazon forest resilience

Supporting Information:

Supporting Information may be found in the online version of this article.

Correspondence to:

L. G. Cattelan,
luisgustavo2000@gmail.com

Citation:

Cattelan, L. G., Hirota, M., Baker, J. C. A., Gonçalves De Souza, J., Aguiar, A. P. D., Oliveira Assis, T., et al. (2026). Impacts of deforestation-driven rainfall reductions on Amazonia forest stability. *Geophysical Research Letters*, *53*, e2026GL122705. https://doi.org/10.1029/2026GL122705

Received 2 APR 2026
Accepted 23 MAY 2026

Author Contributions:

Conceptualization: Luís Gustavo Cattelan, Marina Hirota, Jessica C. A. Baker, Jefferson Gonçalves De Souza, Chris Huntingford, Eddy Robertson, Stephen Sitch, Emanuel Gloor
Funding acquisition: Stephen Sitch, Emanuel Gloor
Methodology: Luís Gustavo Cattelan, Marina Hirota, Jessica C. A. Baker, Jefferson Gonçalves De Souza, Ana Paula Dutra Aguiar, Tainá Oliveira Assis, Chris Huntingford, Stephen Sitch, Emanuel Gloor
Project administration: Stephen Sitch, Emanuel Gloor
Supervision: Stephen Sitch, Emanuel Gloor

1. Introduction

Amazonia plays a vital role in the Earth system by contributing over 20% of global freshwater discharge to the oceans, storing around 100 billion tons of carbon in its above-ground biomass, and is home to more than 40 million people (Flores et al., 2024; Malhi et al., 2008). A defining characteristic of this system is the especially strong coupling between forest cover and rainfall: approximately one-third of the region's precipitation is recycled through the forest's own evapotranspiration (ET), creating a self-sustaining hydrological feedback loop (J. C. A. Baker & Spracklen, 2022; Staal et al., 2018; van der Ent et al., 2014). Forest-atmosphere interactions are particularly important in western Amazonia, where recycled moisture contributes over 50% of total precipitation near the Andes (Zemp et al., 2014). The interdependence of forests and rainfall means that disturbances such as deforestation, forest degradation, or climate change, can trigger cascading effects on the Amazonian hydrological cycle. In general, reduced forest cover lowers ET, leading to a decline in rainfall downwind, which in turn may trigger further reductions in forest cover (Staal et al., 2020). This feedback is central to why Amazonia is

Writing – original draft: Luís Gustavo Cattelan, Jessica C. A. Baker, Jefferson Gonçalves De Souza, Chris Huntingford, Emanuel Gloor
Writing – review & editing: Luís Gustavo Cattelan, Marina Hirota, Jessica C. A. Baker, Jefferson Gonçalves De Souza, Ana Paula Dutra Aguiar, Tainá Oliveira Assis, Chris Huntingford, Eddy Robertson, Stephen Sitch, Emanuel Gloor

considered a tipping element of the Earth system (Lenton et al., 2008; Nobre et al., 2016). Accordingly, exceeding a critical level of forest loss could decrease precipitation sufficiently for the remaining forests to transition rapidly and irreversibly to alternative lower biomass and degraded ecosystems (Flores et al., 2024).

Understanding how water vapor is recycled and moves across Amazonia is key to evaluating the hydrological impacts of forest loss. Atmospheric moisture enters Amazonia from the tropical Atlantic via easterly trade winds and is channeled further inland into the South American Low-Level Jet (SALLJ), which in turn transports large volumes of water vapor toward central and southern South America (Arraut et al., 2012; Jones et al., 2023; Marengo et al., 2004). This flow is modulated by the South American Monsoon System, producing marked seasonal variability (De Carvalho & Cavalcanti, 2016; Vera et al., 2006). Southwestern Amazonia serves as a key moisture source to the La Plata basin via the SALLJ, supplying atmospheric water to agriculturally important regions beyond the basin (Staal et al., 2018). The interactions between atmospheric circulation, vegetation, and topography generate strong spatial gradients in rainfall across the basin. Western Amazonia, where moist air masses are uplifted by the Andes, receives some of the highest precipitation rates in the basin, while southern Amazonia, adjacent to the Cerrado savanna, is drier and rainfall is more seasonal (Costa et al., 2021).

Forests play a critical role buffering the impacts of seasonal rainfall in Amazonia (Mu et al., 2021). During the dry season, forest vegetation continues to transport water from the soil into atmosphere through deep-root access to groundwater, enabling photosynthesis when rainfall is limited. Reduced cloud cover during this period further enhances solar radiation reaching the surface, boosting dry-season ET and productivity (da Rocha et al., 2009; von Randow et al., 2004). These processes are disrupted by deforestation, which has already affected around 20% of the biome with the largest forest losses along the southern and eastern margins of Amazonia, in the "Arc of Deforestation" (Alencar et al., 2020). While small-scale clearings may locally enhance convection (Garcia-Carreras & Parker, 2011; Khanna et al., 2017; Lawrence & Vandecar, 2015) large-scale forest loss significantly reduces ET, leading to rainfall decline both locally and in downwind areas (Smith et al., 2023; D. V. Spracklen et al., 2018). Recent modeling studies estimate that complete Amazonia deforestation could lead to a basin-wide reduction in annual precipitation of $-12 \pm 11\%$ (D. V. Spracklen et al., 2018), potentially pushing some ecosystems beyond their hydrological stability thresholds. Furthermore, some potential vegetation models suggest that deforestation above approximately 40% could threaten the ecosystem stability of remaining forests (Nobre et al., 1991, p. 91; Pires & Costa, 2013; Sampaio et al., 2007). However, substantial uncertainty remains in these projections due to differences in model structure and in the representation of key processes, such as land–atmosphere interactions and detailed representation of regional wind properties that define atmospheric moisture transport. Furthermore, some studies suggest that deforestation alone may not be sufficient to trigger such critical transitions (Lejeune et al., 2015).

Tropical vegetation structure is influenced by various environmental factors including topography, soil properties, and groundwater availability (Bueno et al., 2018; Mattos et al., 2023), although precipitation remains a dominant control (Hirota et al., 2011; Malhi et al., 2009; Staver et al., 2011). Forests, characterized by high tree cover, tend to prevail in regions with high rainfall, whereas savanna-like vegetation with sparse tree cover dominate drier and more seasonal areas. In zones of intermediate precipitation, both forest and savanna-like vegetation can coexist, forming bistable systems. For such systems disturbances, such as fire, drought, or land-use change, can cause vegetation to switch from a forested to a non-forested and degraded state, with limited potential for recovery (Hirota et al., 2011; Zemp et al., 2017). The presence of alternative stable states has been shown to be linked to multiple precipitation indicators in Amazonia, including mean annual precipitation (MAP), dry season length (DSL), and maximum cumulative water deficit (MCWD), which quantifies seasonal water stress (Flores et al., 2024). This framework can be used to assess how changes in rainfall impact forest stability. Furthermore, given the spatial heterogeneity of climate and vegetation across Amazonia, the hydrological consequences of forest loss depend not only on the extent of deforestation but also on where it occurs within the basin (Zemp et al., 2017).

In this study, we assess the extent and locations of where deforestation alters the stability of Amazonia's remaining forests by reducing recycled rainfall and pushing downwind ecosystems towards and beyond critical hydrological thresholds. We specifically ask the question of which parts of Amazonia are at risk solely from deforestation-induced precipitation reductions. We employ an atmosphere moisture tracking approach to quantify precipitation anomalies under an extreme vegetation loss scenario and evaluate whether these changes exceed the stability limits defined by the stable states' framework (Table 1). We identify regions most vulnerable to

Table 1
Threshold Values for Mean Annual Precipitation (MAP), Dry Season Length (DSL), and Maximum Cumulative Water Deficit (MCWD), Based on Flores et al. (2024)

Stability indicator	Savanna-like threshold	Forest threshold	Unit
MAP	1,000	1,800	mm yr^{-1}
DSL	8	5	Months
MCWD	−450	−350	mm (water deficit)

transition, as well as areas where forest conservation or restoration would most effectively enhance downwind ecological stability. By linking vegetation–atmosphere interactions to spatial patterns of climate and land use, our findings offer actionable insights to inform policies aimed at maintaining biodiversity, carbon stocks, water security, and food security through agricultural activities across South America.

2. Methods

2.1. Water Vapor Tracking Model

To investigate the pathways of atmospheric moisture from its origin in evapotranspiration (ET) to its eventual precipitation, we used the Eulerian moisture tracking model WAM-2layers (Kalverla et al., 2024; van der Ent et al., 2010). This model represents the atmosphere as two vertically integrated layers under the assumption of well-mixed conditions. These simplifications allow WAM-2layers to capture essential large-scale moisture transport processes while remaining computationally efficient for high-resolution continental-scale simulations (Kalverla et al., 2024).

For this study, we used version 3 of the WAM-2layers model, which is publicly available on GitHub (Kalverla et al., 2024). The model was driven by meteorological inputs from the ERA5 reanalysis data set (Hersbach et al., 2020) covering the period 2011 to 2020. ERA5 provides hourly data at a spatial resolution of 0.25° × 0.25°, including 22 atmospheric pressure levels and surface variables.

We configured the model over South America by dividing the continent into 1,424 grid cells at 1° × 1° resolution, spanning from the equator to 40°S. For each grid cell and each month, we performed tagged ET simulations, in which all ET from a given cell was tracked through the atmosphere until it precipitated. This produced spatially explicit maps of the downwind destination of moisture from each source region.

To quantify the sensitivity of downwind precipitation to changes in upwind ET, we calculated for each source grid cell the ratio of the total precipitation in downwind sink areas to the average monthly ET in the source grid cell (example in Figure S1 in Supporting Information S1). We then constructed a monthly climatology of these sensitivity matrices over the 2011–2020 period. In the subsequent analysis, the climatological monthly sensitivity is multiplied by the corresponding ET anomaly derived from each LUCC scenario to estimate the resulting change in precipitation.

2.2. Land Use Change Scenarios

To represent present-day vegetation cover across tropical South America, we used the MapBiomas land cover data sets for the year 2020, which provides 30 m spatial resolution (Alencar et al., 2020). We aggregated all native vegetation classes and calculated, for each 0.25° ERA5 grid cell, the fraction of area covered by natural vegetation.

To ensure complete spatial coverage, including regions east of the Amazonia that influence rainfall via easterly moisture transport, we combined two MapBiomas products: the Pan-Amazonia collection, which covers the Amazonia across nine countries (https://amazonia.mapbiomas.org/), and the Brazil collection, which covers the full national territory (https://brasil.mapbiomas.org/; Figure S2 in Supporting Information S1).

We defined two land cover scenarios for analysis. In the deforestation scenario (MapBiomas-all-def), all remaining native vegetation within each grid cell is assumed to be cleared. In the restoration scenario (MapBiomas-all-aff), all non-natural land cover is assumed to regenerate into native vegetation.

To represent a more realistic deforestation scenario, we also used spatially explicit land-use and land-cover change projections from the LUCCME NEXUS data set for Brazil (available at https://zenodo.org/records/16953581). These scenarios were developed using the LuccME modeling framework (Aguiar et al., 2016), which integrates socio-economic and biophysical drivers to simulate land-use dynamics. We focused on changes in natural vegetation cover, defined as the sum of forest vegetation and savanna and grassland vegetation, between 2020 and 2050. Among the available scenarios, we selected the *Historical Trend* (TE) scenario, which assumes the continuation of historical deforestation trends and represents the most aggressive deforestation trajectory (von Randow et al., 2024).

2.3. Evapotranspiration Anomaly

To estimate precipitation changes resulting from land-use transitions, we first generated a map of ET anomalies. Field studies across South America have consistently shown that forests exhibit ET rates approximately 30% higher than those of pasture or croplands during the wet season, and around 50% higher during the dry season (J. C. A. Baker et al., 2021; da Rocha et al., 2009; Nóbrega et al., 2017; Silvério et al., 2015; von Randow et al., 2004). This difference arises from structural and physiological traits of forests—such as higher leaf area index (LAI), deeper rooting systems, and more efficient access to subsurface water—that enable sustained photosynthesis and transpiration, even during the dry season.

For our main scenario, we identified the dry season individually for each grid cell as the three consecutive months with the lowest precipitation, based on climatological means. During this dry season, the evapotranspiration reduction (r_{lucc}) was set to 0.5 to represent stronger contrasts between forested and deforested areas. For the remaining 9 months, corresponding to the wetter part of the year, r_{lucc} was set to 0.3. Additionally, we conducted sensitivity experiments using two alternative scenarios in which r_{lucc} was uniformly set to 50% and 70% throughout the entire year, regardless of season, to test the robustness of our results to different assumptions about ET change (Table S1 in Supporting Information S1).

To represent spatial differences in ET reductions due to land-use change, we applied the following relationship:

$$\Delta \mathrm{ET} = \Delta \mathrm{Lucc} \times r_{\mathrm{lucc}} \times \mathrm{ET}$$

Where ΔLUCC is the fractional change in natural vegetation cover (from 0 to 1), ET is the baseline evapotranspiration. r_{lucc} is the fractional reduction in ET from deforested areas relative to natural vegetation. The result, ΔET, represents the anomaly in ET due to land-use change in millimeters per month.

We assume that changes in ET influence downwind precipitation in a linear manner. For each $1° \times 1°$ grid cell, we compute the monthly ET change and multiply it by the corresponding monthly climatology sensitivity matrix derived from WAM-2layers. This yields an estimate of the precipitation change resulting from land-use transitions of each grid cell. By summing the contributions from all grid cells, we obtain the total precipitation anomaly induced by land-use change across the domain.

2.4. Thresholds and Transitions

To assess the stability of Amazonia under current and altered climate conditions, we used recent published threshold (Flores et al., 2024) (Table 1): for three key hydroclimatic indicators: mean annual precipitation (MAP), maximum cumulative water deficit (MCWD), and dry season length (DSL). These thresholds are used here to characterize *potential vegetation stability*, that is, the climatic suitability for maintaining forest versus low tree-cover states, rather than the actual vegetation currently present in each pixel. In this framework, we do not account for potential non-climatic limitations to forest re-establishment following complete deforestation and instead focus solely on precipitation-driven constraints.

The indicators are derived from monthly climatological precipitation. DSL is defined as months with precipitation less than 100 mm/month. MCWD is defined as the most negative monthly cumulative water balance (precipitation minus evapotranspiration) within a year. We use a fixed ET value of 100 mm month^{-1} to maintain consistency with the threshold definitions adopted in the original threshold study (Flores et al., 2024). Using spatially varying ET would require recalculating the thresholds themselves to ensure methodological consistency.

Each indicator is associated with two thresholds (Table 1): a lower threshold below which vegetation is classified as savanna-like (low tree cover), and an upper threshold above which forest (high tree cover) is the stable state. Values between the two thresholds correspond to a bistable zone, where both forest and savanna-like can be stable depending on local disturbances and feedbacks. Importantly, these stability classes describe the climatic suitability for vegetation states rather than the actual land cover currently observed at each location.

The spatial extent of Amazonia was defined using the boundaries provided by the Red Amazónica de Información Socioambiental Georreferenciada (RAISG, https://www.raisg.org/en/maps/), encompassing approximately 7 million km^2 across nine countries. Additional data sets were used to estimate ET and precipitation anomalies, which were computed by applying the WAM-2layers sensitivity matrices to ET changes (check previous section). Precipitation data were taken from CHIRPS 2.0 (Funk et al., 2015b), consistent with the data set used by Flores et al. (2024) to derive the stability thresholds. Evapotranspiration data were sourced from ERA5, with additional runs using GLEAM v3.8 (Martens et al., 2017) and FLDAS (McNally et al., 2017) data sets (Table S1 in Supporting Information S1). All data correspond to the 2011–2020 period, matching the WAM-2layers simulation timeframe.

We then incorporated precipitation anomalies induced by land-use change and reassessed vegetation stability under these altered conditions. This approach allowed us to map transitions in stability classes across the region. This analysis reflects an immediate post-deforestation state and does not account for subsequent forest regrowth. Accordingly, our framework does not simulate the potential recovery of ET and associated precipitation that could occur through secondary forest development in areas where the climate remains suitable for forest persistence.

2.5. Threat

To generate a continuous stability metric, we first calculated the safety margin for each pixel, defined as the minimum reduction in precipitation required for a transition to occur. Pixels already classified as savanna-like do not have a defined safety margin, as they are below the lower threshold. Conceptually, the safety margin is closely related to *precariousness* in the resilience framework of (B. Walker et al., 2004) as it quantifies how close the system currently is to a critical transition. It is also analogous to *vulnerability* in the IPCC risk framework (Reisinger et al., 2020). Next, we defined a threat metric as the precipitation anomaly induced by deforestation divided by the safety margin. Values above one indicate that the land-use change is sufficient to push the pixel across a stability threshold.

To identify conservation hotspots, we assessed the threat induced by the deforestation of each individual WAM-2layers grid cell. Each cell was assigned a value corresponding to the cumulative threat it caused downwind. These values were log-normalized to improve visualization. For the restoration scenario, we applied the same method but with inverted precipitation anomalies. In this case, threat values are negative, indicating an increase in forest stability by moving further away from transition thresholds.

3. Results

3.1. Patterns of Stability Changes

Using a complete deforestation scenario of all remaining natural vegetation, we first estimate changes in ET and then model the resulting impacts on precipitation (see Methods; Figures S3 and S4 in Supporting Information S1). Our simulations indicate that although a widespread collapse of the Amazonian forests due to reduced rainfall recycling alone is unlikely, significant localized reductions in vegetation stability emerge, particularly along the Arc of Deforestation (Figure 1). While most forested areas remain stable under this scenario—77.9% of Amazonia for MAP, 67.04% for DSL, and 90.9% for MCWD—a substantial fraction transitions to a bistable regime: 10.3% for MAP, 6.3% for DSL, and 2.6% for MCWD (Table S2 in Supporting Information S1).

The spatial patterns of these transitions vary across indicators. MAP-related transitions are concentrated in the southwestern Amazonia, particularly around the state of Rondônia (Figure 1a, Figure S2b in Supporting Information S1). DSL-based transitions occur farther north and east, with notable changes in the eastern Amazonia, especially in Pará (Figure 1b). MCWD-related transitions are located further south relative to the MAP transitions and tend to be less extensive (Figure 1c). All three metrics indicate widespread transitions in Bolivian Amazonia, where 64.12% of pixels experience at least one transition (Figure S5 in Supporting Information S1), while

10.1029/2026GL122705

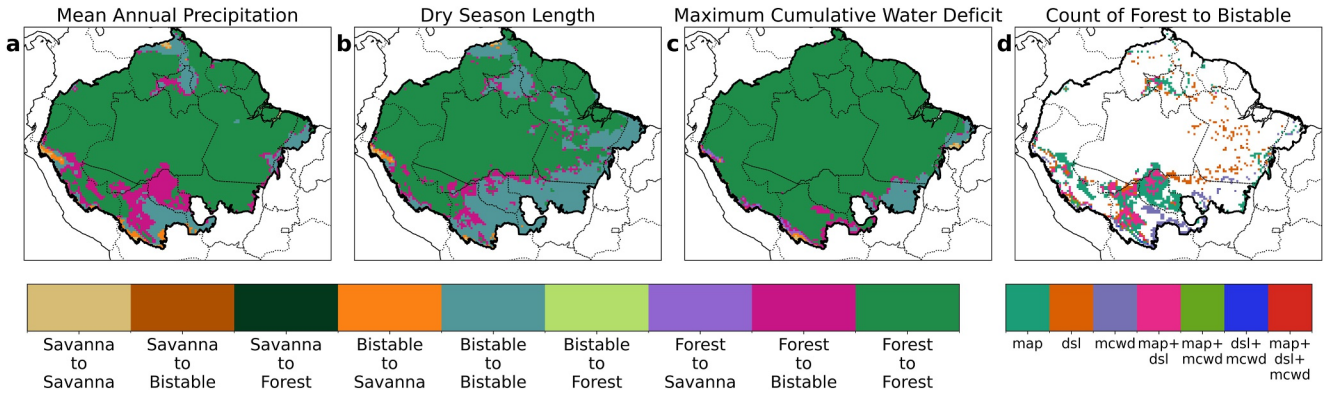

Figure 1. Stability class transitions under extreme deforestation. Vegetation cover stability class changes based on Flores et al. (2024) in response to an extreme deforestation scenario, shown for different precipitation indicators. (a) Mean annual precipitation (MAP). (b) Dry season length (DSL). (c) Maximum cumulative water deficit (MCWD). (d) Combined indicators showing areas transitioning from forest to bistable conditions. Note that the stability classes represent the climate suitability for vegetation cover, not the current vegetation observed in each pixel. Black lines delineate the Amazonia boundary.

Rondônia exhibits the highest proportion, with 80.96% of pixels undergoing a transition. Although most changes are detected by a single metric, approximately 3% of forested pixels exhibit overlapping transitions in two or more variables, highlighting areas of compounded vulnerability (Figure 1d, Table S3 in Supporting Information S1). Conversely, around 52% of the original forest class remains classified as stable across all three metrics, underscoring the persistence of stable forest ecosystems across large parts of the biome.

To move beyond binary classifications of stability, we introduce two complementary metrics: *safety margin* and *threat* (Methods; Figure 2; Figure S6 in Supporting Information S1). The safety margin quantifies the climatic distance to the nearest transition threshold, while the threat metric expresses the size of the precipitation anomaly caused by deforestation relative to that margin. For instance, while the largest precipitation anomalies are found in the wetter western Amazonia (Figures 2b, 2e, and 2g), these areas do not necessarily correspond to the highest threat levels (Figures 2c, 2f, and 2h), owing to their relatively large safety margins. For MCWD, safety margins are smallest in southeastern Amazonia (often below −50 mm, Figure 2g), yet threat levels remain low because anomalies are relatively small in this area (Figure 2i). In contrast, the highest MCWD-based threat values are concentrated along the Brazil–Bolivia border, where high precipitation anomalies coincide with narrow safety margins, resulting in amplified vulnerability.

Importantly, the Threat metric identifies regions that are approaching—but have not exceeded—critical stability thresholds. For instance, under the MAP indicator, extensive areas north of the Arc of Deforestation display threat values around 0.5 (Figure 2c). Although these regions may still be classified as stable in binary transition maps (Figure 1), the elevated threat levels signal proximity to a critical threshold. To assess the robustness of our findings that precipitation changes related to deforestation alone do not cause large-scale transitions, we explored a suite of additional scenarios incorporating more realistic land-use patterns, alternative ET data sets, and varying assumptions about the magnitude of ET reductions following deforestation (Table S1 in Supporting Information S1). Overall, while the intensity of hydrological changes varied across scenarios, the spatial patterns of vulnerability remained consistent (Figure S7 in Supporting Information S1). For instance, under a more extreme assumption of a 70% reduction in ET year-round following deforestation, 26% of forested pixels crossed tipping thresholds for MAP, with a basin-wide average precipitation decline of −18.4%. Conversely, restoration scenarios produced modest but spatially coherent increases in precipitation and stability. This asymmetry is expected, as approximately 80% of Amazônia remains forested. These results highlight that although the magnitude of precipitation change is sensitive to deforestation extent and biophysical assumptions, the locations of the most vulnerable areas remain largely unchanged.

3.2. Forest Conservation and Restoration Hotspots

To identify forests whose deforestation exerts the greatest downwind drying effects, we calculated the cumulative threat generated by each grid cell based on its influence on other forested regions. This approach highlights two prominent source regions of precipitation-mediated threat across all three indicators (Figures 3a–3c). The first

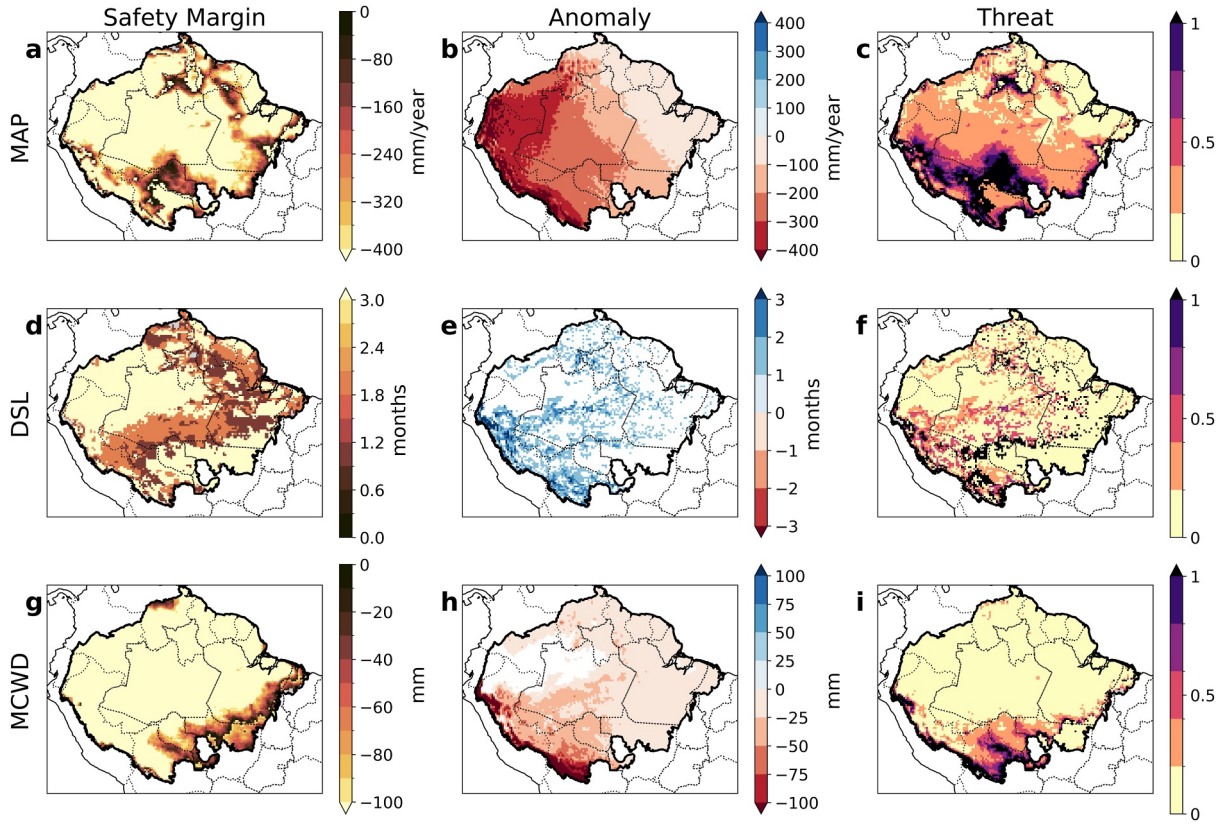

Figure 2. Threat indicators of forest stability under an extreme deforestation scenario. Threat analysis based on the three precipitation indicators of forest stability. (a, d, g) Maps of safety margins, the "distance" of each grid cell from its respective stability threshold. (b, e, h) Projected changes in each indicator due to the deforestation scenario. (c, f, i) Threat metric, calculated as the ratio between anomaly and safety margin. Values greater than 1 indicate a potential transition. Black lines delineate the Amazonia boundary.

cluster is in western Amazonia, along the Brazil–Peru border. The second is in the eastern Amazonia, near the ecotonal region between the Amazonia, Cerrado, and Caatinga biomes. Specifically, the MATOPIBA region, that covers the states of Maranhão, Tocantins, Piauí, and Bahia. From the threat values attributed to grid cells within these clusters (Figure S8 in Supporting Information S1), distinct downwind patterns become evident. The MATOPIBA cluster contributes disproportionately to threat levels in westward areas, strongly impacting large portions of the Arc of Deforestation. In contrast, the western cluster primarily affects regions to its southeast, following prevailing moisture transport pathways associated with the SALLJ. Notably, parts of Rondônia and northern Bolivia are highly affected by both clusters, underscoring their compounded vulnerability to remote deforestation impacts.

We extended our analysis to assess the potential benefits of large-scale restoration by simulating an extreme restoration scenario in which all previously deforested areas are converted back to natural vegetation. While the proportion of pixels shifting from bistable to stable forest conditions is relatively small (approximately −2% of the region; Table S1 in Supporting Information S1), the increase in safety margins is substantial in several areas. In particular, large parts of Mato Grosso and Rondônia exhibit marked reductions in Threat values (below −0.5; Figure S9 in Supporting Information S1), indicating a meaningful movement away from ecological thresholds. This reveals not only a general enhancement in forest resilience but also identifies regions where forest recovery could deliver significant downwind benefits. In particular, eastern Amazonia emerges again as a restoration hotspot (Figures 3d–3f), though slightly shifted westward from the conservation-critical MATOPIBA region. Key areas include the border between the states of Pará and Tocantins in Brazil, where restoration could play a critical role in stabilizing downwind forests.

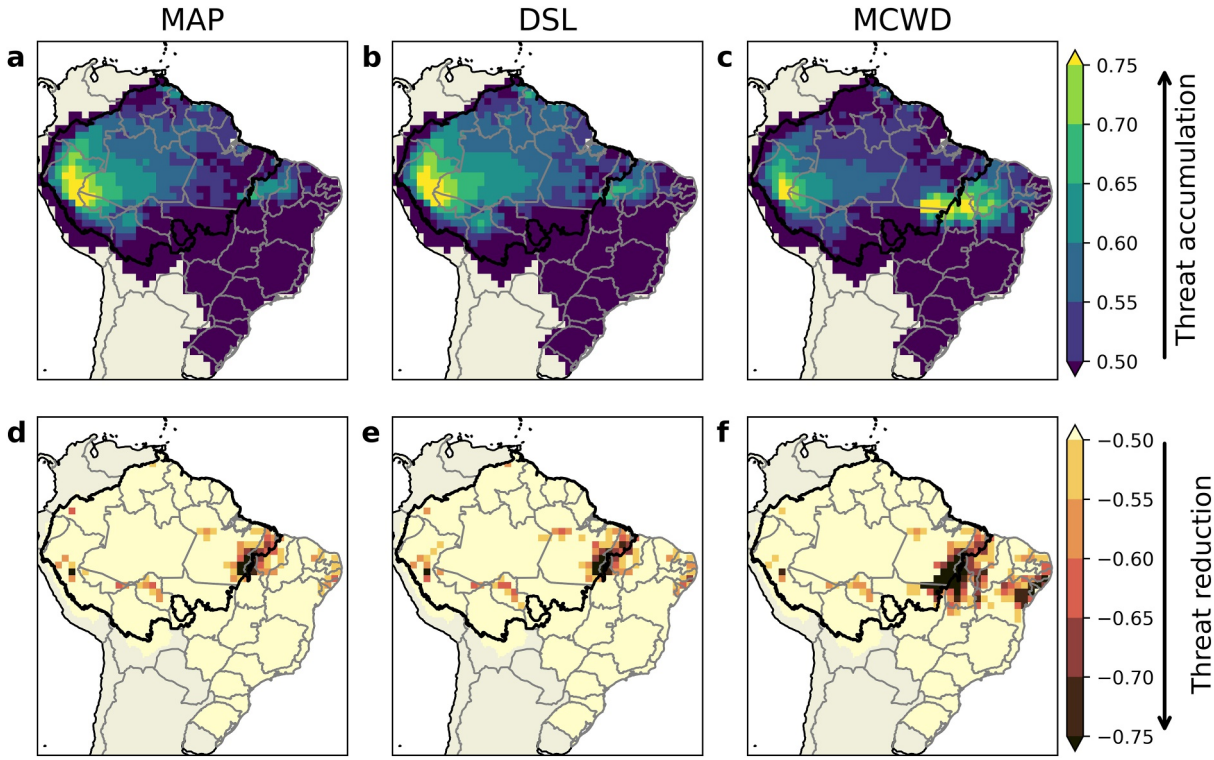

Figure 3. Conservation and Restoration hotspots. (a–c) Spatial distribution of the cumulative Threat generated by the deforestation of each individual grid cell, shown for each precipitation indicator (MAP, DSL, MCWD). (d–f) Spatial distribution of the reduction in Threat resulting from the restoration of each grid cell. Brighter colors in (a–c) indicate areas where deforestation produces stronger negative impacts on downwind forest stability, while darker colors in (d–f) indicate areas where restoration leads to greater improvements in downwind forest stability.

4. Discussion

Our results indicate that, even under an ET scenario equivalent to a complete deforestation, a widespread, basin-wide forest collapse driven solely by deforestation-driven precipitation reductions is unlikely. Across much of the region, post-deforestation climatic conditions remain within the thresholds associated with stable forest states. However, our spatially explicit analysis reveals distinct regional patterns of vulnerability. Although the largest projected rainfall anomalies occur in the wetter western Amazonia, the substantial climatological buffers in these areas for example, high annual precipitation and shorter dry seasons, allow them to retain relative stability. In contrast, regions such as eastern Amazonia are comparatively drier but less dependent on terrestrial moisture recycling. The Arc of Deforestation region stands out as a region where most of the transitions could occur, and this region has already experienced increasing climatic stress in recent decades, with trends closely linked to ongoing forest loss (Butt et al., 2023; Debortoli et al., 2017; Leite-Filho et al., 2019). Critically, parts of southeastern Amazonia are already showing signs of ecological disruption, with evidence that the region has transitioned from a net carbon sink to a carbon source in recent years (Gatti et al., 2021).

Within this Arc, southwestern Amazonia stands out as a hotspot of compounded vulnerability, particularly parts of Rondônia and northern Bolivia. These regions lie close to forest–savanna climatic thresholds and depend heavily on moisture recycling from upwind forested areas, with up to 50% of annual precipitation originating from within-basin evapotranspiration (Zemp et al., 2014). This reliance becomes even more critical during drought years, when oceanic and non-forest moisture sources weaken while recycled moisture from mature forests remains relatively stable, buffering rainfall deficits (Mu et al., 2021). As a result, deforestation in upwind regions can trigger cascading effects, exacerbating water stress in these already fragile areas. Importantly, southwestern forests are not only recipients but also key sources in the continental moisture recycling network, exporting atmospheric moisture to southeastern South America (Staal et al., 2018). Notably, Bolivia experienced severe forest fires in 2024, further highlighting the region's vulnerability to compounding disturbances (Bourgoin et al., 2025).

Despite substantial regional variability, we estimate a basin-wide mean reduction of 203 mm yr^{-1} in MAP under complete deforestation, equivalent to a 9.3% decline relative to baseline climatology. In our most extreme sensitivity scenario, assuming a 70% decrease in ET, rainfall declines reach 19.6%, with approximately 27% of the basin shifting stability class. These values fall within the range of published estimates, including the 12 ± 11% mean reduction reported by D. V. Spracklen and Garcia-Carreras (2015). However, both earlier and more recent studies highlight substantial uncertainty in the magnitude and spatial pattern of precipitation responses, reflecting differences in ET changes, moisture convergence, and circulation adjustments (Alves et al., 2017; Eiras-Barca et al., 2020; Luo et al., 2022; Pires & Costa, 2013; Qin et al., 2025; Sampaio et al., 2007, 2021; Swann et al., 2015; Yoon & Hohenegger, 2025). For instance, some studies identify eastern Amazonia, near the Atlantic, as particularly sensitive to deforestation (Pires & Costa, 2013; Sampaio et al., 2007) whereas others simulate limited changes—similar to our analysis—or even localized precipitation increases in that region Surface roughness and energy partitioning changes can reorganize local and regional circulation, potentially amplifying or compensating drying (Alves et al., 2017; Swann et al., 2015), and high-resolution simulations suggest that circulation adjustments may partially offset ET reductions (Yoon & Hohenegger, 2025). Conversely, observational analyses indicate that precipitation may be more sensitive to forest loss than some climate models suggest (Cui et al., 2026).

By fixing circulation and assuming a linear ET–precipitation relationship, we deliberately isolate the moisture-recycling component and avoid introducing additional model-dependent dynamical uncertainties. To assess how strongly nonlinear precipitation reduction in response to air vapor content reduction (Baudena et al., 2021) would need to be to alter our conclusions, we conducted a scaling analysis using an "Amplification Factor" (Figure S10 in Supporting Information S1), defined as the inverse of Threat. This metric quantifies how much the diagnosed precipitation anomaly would need to be multiplied for a pixel to transition to a drier potential vegetation class. The median amplification factor required for forest-to-bistable transitions is approximately 3 (90th percentile ∼10), and for bistable-to-savanna transitions the 90th percentile reaches ∼15. In precipitation terms, shifting roughly half of the basin into a drier stability class would require MAP reductions on the order of ∼30%, substantially larger than those simulated in most coupled deforestation experiments. Nonetheless, fully coupled, high-resolution Earth system models with improved representation of vegetation and convection process remain essential to better constrain these interacting land–atmosphere feedbacks.

Persistent reductions in rainfall can alter both the functional dynamics and compositional structure of forest ecosystems, even if they do not immediately trigger a shift to a non-forest or low biomass state (Esquivel-Muelbert et al., 2019; Sanchez-Martinez et al., 2025). Chronic hydrological stress reduces soil moisture availability, elevates fire risk, and suppresses biomass productivity (Aragão et al., 2018; Brando et al., 2014). These impacts, while often subtle and cumulative, can erode essential ecosystem functions such as carbon storage, biodiversity support, and hydrological regulation, leading to a progressive loss of forest functionality over time (Lapola et al., 2023), even with the forest adjusting itself. Furthermore, even if precipitation levels remain theoretically sufficient to sustain forest cover, the resulting regrowth following full deforestation would likely be functionally and compositionally distinct from existing forests—substantially less diverse in both flora and fauna.

Another point of caution is that our analysis does not account for ecological heterogeneity in forest drought resilience, which may influence vulnerability across the region (Wunderling et al., 2022). For example, forests in northwestern Amazonia, which experience consistently wet conditions, may appear stable under current climate thresholds but their limited exposure to historical drought may leave them more susceptible to abrupt mortality under novel climate conditions (Tavares et al., 2023). In contrast, southeastern seasonal forests, have evolved traits to cope with regular water deficits and may exhibit greater resilience despite being closer to climatic tipping points (Ciemer et al., 2019).

While deforestation alone may not induce widespread collapse via a reduction in precipitation, it may act synergistically with climate change and forest degradation processes (forest fires, selective logging, edge-effects, fragmentation) to amplify forest vulnerability. Climate models consistently project reductions in precipitation over large portions of the Amazonia under continued global warming, though uncertainty remains across model ensembles (Malhi et al., 2009; Marengo et al., 2024). The combined pressures of land-use change (and associated carbon emissions) and a drying climate may thus lead to more extensive and abrupt ecological transitions than would occur under either stressor in isolation (Nobre et al., 2016).

We highlight two regions where deforestation produces the greatest downwind impacts on Amazonian forest stability: western Amazonia near the Brazil–Peru border and the eastern Amazonia–Cerrado transition, especially the MATOPIBA region. These areas emerge as critical conservation priorities, where protection efforts could have the most significant effect on maintaining ecosystem resilience. The western Amazonia is a key moisture source for southwestern Amazonia via the SALLJ and, due to its relatively mature forest cover and high proportion of protected areas and Indigenous Territories (Figure 2a in Supporting Information S1, (W. S. Walker et al., 2020)), currently helps buffer regional climate stress. In contrast, the MATOPIBA region has seen accelerated deforestation and is experiencing some of Brazil's most intense recent climate stress (Marengo et al., 2022; Silva et al., 2020). Although primarily within the Cerrado biome, MATOPIBA plays a key role in supporting Amazonia rainfall through evapotranspiration that feeds westward moisture transport (Malhado et al., 2010; Spera et al., 2016; D. Spracklen et al., 2012). Yet, the region remains insufficiently protected under current land-use policies, underscoring the need to extend conservation planning beyond the traditional Amazonia boundary.

Shifting the perspective from risks to opportunities, our results also highlight areas where targeted restoration could yield substantial downwind benefits by enhancing regional moisture recycling (J. Baker, 2021; Staal et al., 2024). Eastern Pará state emerges as a strategic zone where restoration could increase downwind rainfall and improve vegetation stability in vulnerable regions. Importantly, field studies show that evapotranspiration and other hydrological functions can recover relatively quickly in secondary forests—within 7–15 years after disturbance (J. C. A. Baker et al., 2025; Brando et al., 2019). This rapid recovery supports the feasibility of forest restoration for climate adaptation, with the potential to enhance the hydrological cycle and increase the local carrying capacity for forests. These findings also carry implications for climate policy, particularly in the context of net-zero targets (Allen et al., 2025). While direct carbon accumulation at restoration sites is typically accounted for, additional carbon uptake in downwind forests—indirectly enhanced through increased rainfall—may also be considered in broader carbon assessments.

Beyond ecological impacts, the hydrological changes induced by land-use change have direct consequences for agriculture and regional economies. In the Arc of Deforestation, less than 10% of croplands are irrigated (Lathuillière et al., 2012; Spera et al., 2016), leaving rainfed agriculture highly exposed to even modest declines in rainfall. Moreover, the impacts of Amazonian deforestation extend far beyond the region. Reductions in atmospheric moisture transport can suppress precipitation across large parts of South America, including the La Plata Basin, a major agricultural hub (Li et al., 2023; O'Connor et al., 2021). Conversely, enhanced rainfall in downwind regions resulting from restoration could improve crop resilience, potentially easing concerns over land competition between forest restoration and food production. These cascading effects underscore the Amazonia's role as a continental-scale hydrological engine, where local land-use decisions influence rainfall and food security across vast distances.

5. Conclusions

In conclusion, our analysis suggests that precipitation changes caused by deforestation alone via the forest-rainfall feedback are unlikely to trigger a large-scale and systemic tipping point across Amazonia. While forest loss disrupts moisture recycling and reduces regional rainfall, the resulting climatic conditions generally remain within the bounds of the forest state. Basin-wide stability transitions would require substantially larger precipitation declines, indicating that strong nonlinear amplification or major circulation adjustments would be necessary to induce widespread tipping under large-scale deforestation. Nonetheless, southwestern regions are particularly vulnerable due to their proximity to rainfall thresholds and reliance on upwind moisture sources. Even without a critical transition, these precipitation changes can gradually erode key ecosystem functions such as carbon storage, biodiversity support, and hydrological regulation, especially under persistent water stress. When combined with other stressors such as fire, degradation, and climate change, these impacts may accelerate forest decline and lead to more widespread and abrupt ecological transitions.

We identify two spatial priorities for intervention: conservation hotspots like the western Amazonia and the MATOPIBA region, where deforestation has strong downwind drying effects; and restoration hotspots in eastern Pará, where restoration could enhance moisture recycling and climate resilience. Beyond forest health, rainfall reductions pose broader socio-economic risks—threatening rainfed agriculture, water availability, and energy production across regions like the Arc of Deforestation and La Plata Basin. These findings underscore the need for

integrated, transboundary land-use planning that addresses both ecological transitions and human vulnerabilities, recognizing Amazonia as a deeply interconnected socio-ecological system.

Conflict of Interest

The authors declare no conflicts of interest relevant to this study.

Availability Statement

All data sets used in this study are publicly available. CHIRPS precipitation data are available through Funk et al. (2015a). ERA5 reanalysis data are available through Hersbach et al. (2023). Land-cover data from MapBiomas are available through the MapBiomas Project (2023). LUCCME land-use scenarios are archived at Aguiar et al. (2025). The WAM-2layers moisture tracking model is openly available through van der Ent et al. (2026).

Acknowledgments

We thank Ruud van der Ent and the developers of the WAM-2layers Python package for making the model openly accessible and user-friendly. We are also grateful to Caio Mattos for valuable and insightful discussions throughout this work. We thank the two anonymous reviewers for their constructive comments and suggestions, which helped improve the manuscript. The development of this research has been supported by the Newton Fund through the Met Office (DN694878) Climate Science for Service Partnership Brazil (CSSP Brazil). In addition, EG and SS were supported by UKRI NERC funding (NE/X019055/1 Amazon-SOS). For the purpose of open access, the authors have applied a "Creative Commons Attribution (CC BY) license to any Author Accepted Manuscript version arising." M. H. acknowledges support from the Serrapilheira Institute (Grant 1709-18983). J.B. was supported by a UK Research and Innovation (UKRI) Future Leaders Fellowship (Grant Ref: MR/X034097/1).

References

Aguiar, A. P. D., et al. (2025). LuccME Nexus sustainable land use and land cover change scenarios for Brazil 2050 [Dataset]. *Zenodo*. https://doi.org/10.5281/zenodo.16953581

Aguiar, A. P. D., Vieira, I. C. G., Assis, T. O., Dalla-Nora, E. L., Toledo, P. M., Oliveira Santos-Junior, R. A., et al. (2016). Land use change emission scenarios: Anticipating a forest transition process in the Brazilian Amazon. *Global Change Biology*, *22*(5), 1821–1840. https://doi.org/10.1111/gcb.13134

Alencar, A., Z. Shimbo, J., Lenti, F., Balzani Marques, C., Zimbres, B., Rosa, M., et al. (2020). Mapping three decades of changes in the Brazilian Savanna Native Vegetation Using Landsat Data Processed in the Google Earth Engine Platform. *Remote Sensing*, *12*(6), 924. https://doi.org/10.3390/rs12060924

Allen, M. R., Frame, D. J., Friedlingstein, P., Gillett, N. P., Grassi, G., Gregory, J. M., et al. (2025). Geological Net Zero and the need for disaggregated accounting for carbon sinks. *Nature*, *638*(8050), 343–350. https://doi.org/10.1038/s41586-024-08326-8

Alves, L. M., Marengo, J. A., Fu, R., & Bombardi, R. J. (2017). Sensitivity of Amazon regional climate to deforestation. *American Journal of Climate Change*, *6*(1), 75–98. https://doi.org/10.4236/ajcc.2017.61005

Aragão, L. E. O. C., Anderson, L. O., Fonseca, M. G., Rosan, T. M., Vedovato, L. B., Wagner, F. H., et al. (2018). 21st Century drought-related fires counteract the decline of Amazon deforestation carbon emissions. *Nature Communications*, *9*(1), 536. https://doi.org/10.1038/s41467-017-02771-y

Arraut, J. M., Nobre, C., Barbosa, H. M. J., Obregon, G., & Marengo, J. (2012). Aerial Rivers and Lakes: Looking at large-scale moisture transport and its relation to Amazonia and to subtropical rainfall in South America. *Journal of Climate*, *25*(2), 543–556. https://doi.org/10.1175/2011JCLI4189.1

Baker, J. (2021). Planting trees to combat drought. *Nature Geoscience*, *14*(7), 1–2. https://doi.org/10.1038/s41561-021-00787-0

Baker, J. C. A., Adami, M., Silva-Junior, C. H. L., Sadeck, L. W. R., Smith, C., Heinrich, V. H. A., et al. (2025). Climate benefits of Amazon secondary forests—Recent advances and research needs. *Environmental Research Letters*, *20*(4), 043001. https://doi.org/10.1088/1748-9326/adb984

Baker, J. C. A., Garcia-Carreras, L., Gloor, M., Marsham, J. H., Buermann, W., Da Rocha, H. R., et al. (2021). Evapotranspiration in the Amazon: Spatial patterns, seasonality, and recent trends in observations, reanalysis, and climate models. *Hydrology and Earth System Sciences*, *25*(4), 2279–2300. https://doi.org/10.5194/hess-25-2279-2021

Baker, J. C. A., & Spracklen, D. V. (2022). Divergent representation of precipitation recycling in the Amazon and the Congo in CMIP6 Models. *Geophysical Research Letters*, *49*(10), e2021GL095136. https://doi.org/10.1029/2021GL095136

Baudena, M., Tuinenburg, O. A., Ferdinand, P. A., & Staal, A. (2021). Effects of land-use change in the Amazon on precipitation are likely underestimated. *Global Change Biology*, *27*(21), 5580–5587. https://doi.org/10.1111/gcb.15810

Bourgoin, C., Beuchle, R., Branco, A., Carreiras, J., Ceccherini, G., Oom, D., et al. (2025). Extensive fire-driven degradation in 2024 marks worst Amazon forest disturbance in over two decades. *Remote Sensing: Terrestrial*. https://doi.org/10.5194/egusphere-2025-1823

Brando, P. M., Balch, J. K., Nepstad, D. C., Morton, D. C., Putz, F. E., Coe, M. T., et al. (2014). Abrupt increases in Amazonian tree mortality due to drought–fire interactions. *Proceedings of the National Academy of Sciences*, *111*(17), 6347–6352. https://doi.org/10.1073/pnas.1305499111

Brando, P. M., Silvério, D., Maracahipes-Santos, L., Oliveira-Santos, C., Levick, S. R., Coe, M. T., et al. (2019). Prolonged tropical forest degradation due to compounding disturbances: Implications for CO_2 and H_2O fluxes. *Global Change Biology*, *25*(9), 2855–2868. https://doi.org/10.1111/gcb.14659

Bueno, M. L., Dexter, K. G., Pennington, R. T., Pontara, V., Neves, D. M., Ratter, J. A., & de Oliveira-Filho, A. T. (2018). The environmental triangle of the Cerrado Domain: Ecological factors driving shifts in tree species composition between forests and savannas. *Journal of Ecology*, *106*(5), 2109–2120. https://doi.org/10.1111/1365-2745.12969

Butt, E. W., Baker, J. C. A., Bezerra, F. G. S., von Randow, C., Aguiar, A. P. D., & Spracklen, D. V. (2023). Amazon deforestation causes strong regional warming. *Proceedings of the National Academy of Sciences*, *120*(45), e2309123120. https://doi.org/10.1073/pnas.2309123120

Ciemer, C., Boers, N., Hirota, M., Kurths, J., Müller-Hansen, F., Oliveira, R. S., & Winkelmann, R. (2019). Higher resilience to climatic disturbances in tropical vegetation exposed to more variable rainfall. *Nature Geoscience*, *12*(3), 174–179. https://doi.org/10.1038/s41561-019-0312-z

Costa, M. H., Borma, L. S., Espinoza, J.-C., Marcia, M., Marengo, J. A., Marra, D. M., et al. (2021). Chapter 5: The Physical hydroclimate system of the Amazon. In *Science Panel for the Amazon, Amazon Assessment Report 2021* (1st ed.). UN Sustainable Development Solutions Network (SDSN). https://doi.org/10.55161/HTSD9250

Cui, J., Piao, S., Huntingford, C., Wang, T., & Spracklen, D. V. (2026). Historical deforestation drives strong rainfall decline across the southern Amazon basin. *Nature Communications*, *17*(1), 1642. https://doi.org/10.1038/s41467-026-68361-z

da Rocha, H. R., Manzi, A. O., Cabral, O. M., Miller, S. D., Goulden, M. L., Saleska, S. R., et al. (2009). Patterns of water and heat flux across a biome gradient from tropical forest to savanna in Brazil. *Journal of Geophysical Research*, *114*(G1). https://doi.org/10.1029/2007JG000640

Debortoli, N. S., Dubreuil, V., Hirota, M., Filho, S. R., Lindoso, D. P., & Nabucet, J. (2017). Detecting deforestation impacts in Southern Amazonia rainfall using rain gauges: Are rain gauges able to detect deforestation impacts in precipitation? *International Journal of Climatology*, *37*(6), 2889–2900. https://doi.org/10.1002/joc.4886

De Carvalho, L. M. V., & Cavalcanti, I. F. A. (2016). The South American Monsoon System (SAMS). In L. M. V. De Carvalho & C. Jones (Eds.), *The monsoons and climate change* (pp. 121–148). Springer International Publishing. https://doi.org/10.1007/978-3-319-21650-8_6

Eiras-Barca, J., Dominguez, F., Yang, Z., Chug, D., Nieto, R., Gimeno, L., & Miguez-Macho, G. (2020). Changes in South American hydroclimate under projected Amazonian deforestation. *Annals of the New York Academy of Sciences*, *1472*(1), 104–122. https://doi.org/10.1111/nyas.14364

Esquivel-Muelbert, A., Baker, T. R., Dexter, K. G., Lewis, S. L., Brienen, R. J., Feldpausch, T. R., et al. (2019). Compositional response of Amazon forests to climate change. *Global Change Biology*, *25*(1), 39–56. https://doi.org/10.1111/gcb.14413

Flores, B. M., Montoya, E., Sakschewski, B., Nascimento, N., Staal, A., Betts, R. A., et al. (2024). Critical transitions in the Amazon forest system. *Nature*, *626*(7999), 555–564. Article 7999. https://doi.org/10.1038/s41586-023-06970-0

Funk, C., Peterson, P., Landsfeld, M., Pedreros, D., Verdin, J., Shukla, S., et al. (2015a). CHIRPS [Dataset]. *Scientific Data*, *2*, 150066. https://doi.org/10.1038/sdata.2015.66

Funk, C., Peterson, P., Landsfeld, M., Pedreros, D., Verdin, J., Shukla, S., et al. (2015b). The climate hazards infrared precipitation with stations—A new environmental record for monitoring extremes. *Scientific Data*, *2*(1), 150066. https://doi.org/10.1038/sdata.2015.66

Garcia-Carreras, L., & Parker, D. J. (2011). How does local tropical deforestation affect rainfall? *Geophysical Research Letters*, *38*(19). https://doi.org/10.1029/2011GL049099

Gatti, L. V., Basso, L. S., Miller, J. B., Gloor, M., Gatti Domingues, L., Cassol, H. L. G., et al. (2021). Amazonia as a carbon source linked to deforestation and climate change. *Nature*, *595*(7867), 388–393. https://doi.org/10.1038/s41586-021-03629-6

Hersbach, H., Bell, B., Berrisford, P., Biavati, G., Horányi, A., Muñoz Sabater, J., et al. (2023). ERA5 hourly data on pressure levels from 1940 to present [Dataset]. *Copernicus Climate Change Service (C3S) Climate Data Store*. https://doi.org/10.24381/cds.bd0915c6

Hersbach, H., Bell, B., Berrisford, P., Hirahara, S., Horányi, A., Muñoz-Sabater, J., et al. (2020). The ERA5 global reanalysis. *Quarterly Journal of the Royal Meteorological Society*, *146*(730), 1999–2049. https://doi.org/10.1002/qj.3803

Hirota, M., Holmgren, M., Van Nes, E. H., & Scheffer, M. (2011). Global resilience of tropical forest and savanna to critical transitions. *Science*, *334*(6053), 232–235. https://doi.org/10.1126/science.1210657

Jones, C., Mu, Y., Carvalho, L. M. V., & Ding, Q. (2023). The South America Low-Level Jet: Form, variability and large-scale forcings. *npj Climate and Atmospheric Science*, *6*(1), 1–11. https://doi.org/10.1038/s41612-023-00501-4

Kalverla, P., Benedict, I., Weijenborg, C., & Van Der Ent, R. J. (2024). Atmospheric moisture tracking with WAM2layers v3. *Atmospheric sciences*. https://doi.org/10.5194/egusphere-2024-3401

Khanna, J., Medvigy, D., Fueglistaler, S., & Walko, R. (2017). Regional dry-season climate changes due to three decades of Amazonian deforestation. *Nature Climate Change*, *7*(3), 200–204. https://doi.org/10.1038/nclimate3226

Lapola, D. M., Pinho, P., Barlow, J., Aragão, L. E. O. C., Berenguer, E., Carmenta, R., et al. (2023). The drivers and impacts of Amazon forest degradation. *Science*, *379*(6630), eabp8622. https://doi.org/10.1126/science.abp8622

Lathuillière, M. J., Johnson, M. S., & Donner, S. D. (2012). Water use by terrestrial ecosystems: Temporal variability in rainforest and agricultural contributions to evapotranspiration in Mato Grosso, Brazil. *Environmental Research Letters*, *7*(2), 024024. https://doi.org/10.1088/1748-9326/7/2/024024

Lawrence, D., & Vandecar, K. (2015). Effects of tropical deforestation on climate and agriculture. *Nature Climate Change*, *5*(1), 27–36. Article 1. https://doi.org/10.1038/nclimate2430

Leite-Filho, A. T., de Sousa Pontes, V. Y., & Costa, M. H. (2019). Effects of deforestation on the onset of the rainy season and the duration of dry spells in Southern Amazonia. *Journal of Geophysical Research: Atmospheres*, *124*(10), 5268–5281. https://doi.org/10.1029/2018JD029537

Lejeune, Q., Davin, E. L., Guillod, B. P., & Seneviratne, S. I. (2015). Influence of Amazonian deforestation on the future evolution of regional surface fluxes, circulation, surface temperature and precipitation. *Climate Dynamics*, *44*(9), 2769–2786. https://doi.org/10.1007/s00382-014-2203-8

Lenton, T. M., Held, H., Kriegler, E., Hall, J. W., Lucht, W., Rahmstorf, S., & Schellnhuber, H. J. (2008). Tipping elements in the Earth's climate system. *Proceedings of the National Academy of Sciences*, *105*(6), 1786–1793. https://doi.org/10.1073/pnas.0705414105

Li, H., Keune, J., Smessaert, F., Nieto, R., Gimeno, L., & Miralles, D. G. (2023). Land–atmosphere feedbacks contribute to crop failure in global rainfed breadbaskets. *npj Climate and Atmospheric Science*, *6*(1), 1–9. https://doi.org/10.1038/s41612-023-00375-6

Luo, X., Ge, J., Guo, W., Fan, L., Chen, C., Liu, Y., & Yang, L. (2022). The biophysical impacts of deforestation on precipitation: Results from the CMIP6 model intercomparison. https://doi.org/10.1175/JCLI-D-21-0689.1

Malhado, A. C. M., Pires, G. F., & Costa, M. H. (2010). Cerrado conservation is essential to protect the Amazon Rainforest. *Ambio*, *39*(8), 580–584. https://doi.org/10.1007/s13280-010-0084-6

Malhi, Y., Aragão, L. E. O. C., Galbraith, D., Huntingford, C., Fisher, R., Zelazowski, P., et al. (2009). Exploring the likelihood and mechanism of a climate-change-induced dieback of the Amazon rainforest. *Proceedings of the National Academy of Sciences*, *106*(49), 20610–20615. https://doi.org/10.1073/pnas.0804619106

Malhi, Y., Roberts, J. T., Betts, R. A., Killeen, T. J., Li, W., & Nobre, C. A. (2008). Climate change, deforestation, and the fate of the Amazon. *Science*, *319*(5860), 169–172. https://doi.org/10.1126/science.1146961

MapBiomas Project. (2023). Collection 8 of Brazilian land cover and land use map series [Dataset]. Retrieved from https://brasil.mapbiomas.org/en/colecoes-mapbiomas/

Marengo, J. A., Espinoza, J.-C., Fu, R., Jimenez Muñoz, J. C., Alves, L. M., Da Rocha, H. R., & Schöngart, J. (2024). Long-term variability, extremes and changes in temperature and hydrometeorology in the Amazon region: A review. *Acta Amazonica*, *54*(spe1), e54es22098. https://doi.org/10.1590/1809-4392202200980

Marengo, J. A., Jimenez, J. C., Espinoza, J.-C., Cunha, A. P., & Aragão, L. E. O. (2022). Increased climate pressure on the agricultural Frontier in the Eastern Amazonia–Cerrado transition zone. *Scientific Reports*, *12*(1), 457. https://doi.org/10.1038/s41598-021-04241-4

Marengo, J. A., Soares, W. R., Saulo, C., & Nicolini, M. (2004). Climatology of the low-level Jet East of the Andes as derived from the NCEP–NCAR reanalyses: Characteristics and Temporal Variability. *Journal of Climate*, *17*(12), 2261–2280. https://doi.org/10.1175/1520-0442(2004)017<2261:cotlje>2.0.co;2

Martens, B., Miralles, D. G., Lievens, H., van der Schalie, R., de Jeu, R. A. M., Fernández-Prieto, D., et al. (2017). GLEAM v3: Satellite-based land evaporation and root-zone soil moisture. *Geoscientific Model Development*, *10*(5), 1903–1925. https://doi.org/10.5194/gmd-10-1903-2017

Mattos, C. R. C., Hirota, M., Oliveira, R. S., Flores, B. M., Miguez-Macho, G., Pokhrel, Y., & Fan, Y. (2023). Double stress of waterlogging and drought drives forest–Savanna coexistence. *Proceedings of the National Academy of Sciences*, *120*(33), e2301255120. https://doi.org/10.1073/pnas.2301255120

McNally, A., Arsenault, K., Kumar, S., Shukla, S., Peterson, P., Wang, S., et al. (2017). A land data assimilation system for sub-Saharan Africa food and water security applications. *Scientific Data*, *4*(1), 170012. https://doi.org/10.1038/sdata.2017.12

Mu, Y., Biggs, T. W., & De Sales, F. (2021). Forests mitigate drought in an agricultural region of the Brazilian Amazon: Atmospheric moisture tracking to identify critical source areas. *Geophysical Research Letters*, *48*(5), e2020GL091380. https://doi.org/10.1029/2020GL091380

Nobre, C. A., Sampaio, G., Borma, L. S., Castilla-Rubio, J. C., Silva, J. S., & Cardoso, M. (2016). Land-use and climate change risks in the Amazon and the need of a novel sustainable development paradigm. *Proceedings of the National Academy of Sciences*, *113*(39), 10759–10768. https://doi.org/10.1073/pnas.1605516113

Nobre, C. A., Sellers, P. J., & Shukla, J. (1991). Amazonian deforestation and regional climate change. *Journal of Climate*, *4*(10), 957–988. https://doi.org/10.1175/1520-0442(1991)004<0957:adarcc>2.0.co;2

Nóbrega, R. L. B., Guzha, A. C., Torres, G. N., Kovacs, K., Lamparter, G., Amorim, R. S. S., et al. (2017). Effects of conversion of native Cerrado vegetation to pasture on soil hydro-physical properties, evapotranspiration and streamflow on the Amazonian agricultural Frontier. *PLoS One*, *12*(6), e0179414. https://doi.org/10.1371/journal.pone.0179414

O'Connor, J. C., Santos, M. J., Dekker, S. C., Rebel, K. T., & Tuinenburg, O. A. (2021). Atmospheric moisture contribution to the growing season in the Amazon arc of deforestation. *Environmental Research Letters*, *16*(8), 084026. https://doi.org/10.1088/1748-9326/ac12f0

Pires, G. F., & Costa, M. H. (2013). Deforestation causes different subregional effects on the Amazon bioclimatic equilibrium. *Geophysical Research Letters*, *40*(14), 3618–3623. https://doi.org/10.1002/grl.50570

Qin, Y., Wang, D., Ziegler, A. D., Fu, B., & Zeng, Z. (2025). Impact of Amazonian deforestation on precipitation reverses between seasons. *Nature*, *639*(8053), 102–108. https://doi.org/10.1038/s41586-024-08570-y

Reisinger, A., Howden, M., Vera, C., Mach, K. J., Mintenbeck, K., O'Neill, B., et al. (2020). *The concept of risk in the IPCC Sixth Assessment Report: A summary of crossWorking Group discussions*. Intergovernmental Panel on Climate Change.

Sampaio, G., Nobre, C., Costa, M. H., Satyamurty, P., Soares-Filho, B. S., & Cardoso, M. (2007). Regional climate change over eastern Amazonia caused by pasture and soybean cropland expansion. *Geophysical Research Letters*, *34*(17). https://doi.org/10.1029/2007GL030612

Sampaio, G., Shimizu, M. H., Guimarães-Júnior, C. A., Alexandre, F., Guatura, M., Cardoso, M., et al. (2021). CO_2 physiological effect can cause rainfall decrease as strong as large-scale deforestation in the Amazon. *Biogeosciences*, *18*(8), 2511–2525. https://doi.org/10.5194/bg-18-2511-2021

Sanchez-Martinez, P., Martius, L. R., Bittencourt, P., Silva, M., Binks, O., Coughlin, I., et al. (2025). Amazon rainforest adjusts to long-term experimental drought. *Nature Ecology & Evolution*, *9*(6), 970–979. https://doi.org/10.1038/s41559-025-02702-x

Silva, P. S., Rodrigues, J. A., Santos, F. L. M., Pereira, A. A., Nogueira, J., DaCamara, C. C., & Libonati, R. (2020). Drivers of burned area patterns in Cerrado: The case of matopiba region. In *The International Archives of the Photogrammetry, Remote Sensing and Spatial Information Sciences, XLII-3/W12-2020* (pp. 135–140). https://doi.org/10.5194/isprs-archives-XLII-3-W12-2020-135-2020

Silvério, D. V., Brando, P. M., Macedo, M. N., Beck, P. S. A., Bustamante, M., & Coe, M. T. (2015). Agricultural expansion dominates climate changes in southeastern Amazonia: The overlooked non-GHG forcing. *Environmental Research Letters*, *10*(10), 104015. https://doi.org/10.1088/1748-9326/10/10/104015

Smith, C., Baker, J. C. A., & Spracklen, D. V. (2023). Tropical deforestation causes large reductions in observed precipitation. *Nature*, *615*(7951), 270–275. https://doi.org/10.1038/s41586-022-05690-1

Spera, S. A., Galford, G. L., Coe, M. T., Macedo, M. N., & Mustard, J. F. (2016). Land-use change affects water recycling in Brazil's last agricultural Frontier. *Global Change Biology*, *22*(10), 3405–3413. https://doi.org/10.1111/gcb.13298

Spracklen, D., Arnold, S., & Taylor, C. (2012). Observations of increased tropical rainfall preceded by air passage over forests. *Nature*, *489*(7415), 282–285. https://doi.org/10.1038/nature11390

Spracklen, D. V., Baker, J. C. A., Garcia-Carreras, L., & Marsham, J. H. (2018). The effects of tropical vegetation on rainfall. *Annual Review of Environment and Resources*, *43*(1), 193–218. https://doi.org/10.1146/annurev-environ-102017-030136

Spracklen, D. V., & Garcia-Carreras, L. (2015). The impact of Amazonian deforestation on Amazon basin rainfall. *Geophysical Research Letters*, *42*, 9546–9552. https://doi.org/10.1002/2015GL066063

Staal, A., Flores, B. M., Aguiar, A. P. D., Bosmans, J. H. C., Fetzer, I., & Tuinenburg, O. A. (2020). Feedback between drought and deforestation in the Amazon. *Environmental Research Letters*, *15*(4), 044024. https://doi.org/10.1088/1748-9326/ab738e

Staal, A., Theeuwen, J. J. E., Wang-Erlandsson, L., Wunderling, N., & Dekker, S. C. (2024). Targeted rainfall enhancement as an objective of forestation. *Global Change Biology*, *30*(1), e17096. https://doi.org/10.1111/gcb.17096

Staal, A., Tuinenburg, O. A., Bosmans, J. H. C., Holmgren, M., van Nes, E. H., Scheffer, M., et al. (2018). Forest-rainfall cascades buffer against drought across the Amazon. *Nature Climate Change*, *8*(6), 539–543. Article 6. https://doi.org/10.1038/s41558-018-0177-y

Staver, A. C., Archibald, S., & Levin, S. A. (2011). The global extent and determinants of savanna and forest as alternative biome states. *Science*, *334*(6053), 230–232. https://doi.org/10.1126/science.1210465

Swann, A. L. S., Longo, M., Knox, R. G., Lee, E., & Moorcroft, P. R. (2015). Future deforestation in the Amazon and consequences for South American climate. *Agricultural and Forest Meteorology*, *214–215*, 12–24. https://doi.org/10.1016/j.agrformet.2015.07.006

Tavares, J. V., Oliveira, R. S., Mencuccini, M., Signori-Müller, C., Pereira, L., Diniz, F. C., et al. (2023). Basin-wide variation in tree hydraulic safety margins predicts the carbon balance of Amazon forests. *Nature*, *617*(7959), 111–117. https://doi.org/10.1038/s41586-023-05971-3

van der Ent, R. J., Benedict, I. B., Weijenborg, C., Schilperoort, B., Liu, Y., Bakels, L., et al. (2026). WAM2layers [Computer software]. *Zenodo*. https://doi.org/10.5281/zenodo.19135489

van der Ent, R. J., Savenije, H. H. G., Schaefli, B., & Steele-Dunne, S. C. (2010). Origin and fate of atmospheric moisture over continents. *Water Resources Research*, *46*(9). https://doi.org/10.1029/2010WR009127

van der Ent, R. J., Wang-Erlandsson, L., Keys, P. W., & Savenije, H. H. G. (2014). Contrasting roles of interception and transpiration in the hydrological cycle—Part 2: Moisture recycling. *Earth System Dynamics*, *5*(2), 471–489. https://doi.org/10.5194/esd-5-471-2014

Vera, C., Higgins, W., Amador, J., Ambrizzi, T., Garreaud, R., Gochis, D., et al. (2006). Toward a unified view of the American Monsoon Systems. *Journal of Climate*, *19*(20), 4977–5000. https://doi.org/10.1175/JCLI3896.1

von Randow, C., Aguiar, A. P. D., Bezerra, F. G. S., Martins, M. A., Miranda, M., Sousa Silvino, A., et al. (2024). Relatório Técnico Projeto Nexus. *INPE*. https://nexus.ccst.inpe.br/wp-content/uploads/2024/10/Nexus-Relatorio-Tecnico.pdf

von Randow, C., Manzi, A. O., Kruijt, B., de Oliveira, P. J., Zanchi, F. B., Silva, R. L., et al. (2004). Comparative measurements and seasonal variations in energy and carbon exchange over forest and pasture in South West Amazonia. *Theoretical and Applied Climatology*, *78*(1), 5–26. https://doi.org/10.1007/s00704-004-0041-z

Walker, B., Holling, C. S., Carpenter, S., & Kinzig, A. (2004). Ecology and society: Resilience, adaptability and transformability in social–ecological systems. *Ecology and Society*, *9*(2), art5. https://doi.org/10.5751/ES-00650-090205

Walker, W. S., Gorelik, S. R., Baccini, A., Aragon-Osejo, J. L., Josse, C., Meyer, C., et al. (2020). The role of forest conversion, degradation, and disturbance in the carbon dynamics of Amazon indigenous territories and protected areas. *Proceedings of the National Academy of Sciences*, *117*(6), 3015–3025. https://doi.org/10.1073/pnas.1913321117

Wunderling, N., Staal, A., Sakschewski, B., Hirota, M., Tuinenburg, O. A., Donges, J. F., et al. (2022). Recurrent droughts increase risk of cascading tipping events by outpacing adaptive capacities in the Amazon rainforest. *Proceedings of the National Academy of Sciences*, *119*(32), e2120777119. https://doi.org/10.1073/pnas.2120777119

Yoon, A., & Hohenegger, C. (2025). Muted Amazon rainfall response to deforestation in a global storm-resolving model. *Geophysical Research Letters*, *52*(4), e2024GL110503. https://doi.org/10.1029/2024GL110503

Zemp, D. C., Schleussner, C.-F., Barbosa, H. M. J., & Rammig, A. (2017). Deforestation effects on Amazon forest resilience. *Geophysical Research Letters*, *44*(12), 6182–6190. https://doi.org/10.1002/2017GL072955

Zemp, D. C., Schleussner, C.-F., Barbosa, H. M. J., van der Ent, R. J., Donges, J. F., Heinke, J., et al. (2014). On the importance of cascading moisture recycling in South America. *Atmospheric Chemistry and Physics*, *14*(23), 13337–13359. https://doi.org/10.5194/acp-14-13337-2014